A Structural Characterization of the Interactions between Titin Z-Repeats and the α-Actinin C-Terminal Domain

C. Joseph,[‡] G. Stier,[§] R. O'Brien,[||] A. S. Politou,[⊥] R. A. Atkinson,[‡] A. Bianco,[#,@] J. E. Ladbury,[||] S. R. Martin,[‡] and A. Pastore*,[‡]

NIMR, The Ridgeway, London NW7 1AA, U.K., EMBL, Meyerhofstrasse 1, D-69017 Heidelberg, Germany, University College London, London WC1E 6BT, U.K., Medical School, University of Ioannina, Ioannina 65110, Greece, and Institut für Organische Chemie, Universität Tübingen, D-72076 Tübingen, Germany

Received November 30, 2000; Revised Manuscript Received January 22, 2001

ABSTRACT: Titin and α-actinin, two modular muscle proteins, are with actin the major components of the Z-band in vertebrate striated muscles where they serve to organize the antiparallel actin filament arrays in adjacent sarcomeres and to transmit tension between sarcomeres during activation. Interactions between titin and α-actinin have been mainly localized in a 45-amino acid multiple motif (Z-repeat) in the N-terminal region of titin and the C-terminal region of α-actinin. In this study, we provide the first quantitative characterization of α-actinin−Z-repeat recognition and dissect the interaction to its minimal units. Different complementary techniques, such as circular dichroism, calorimetry, and nuclear magnetic spectroscopy, were used. Two overlapping α-actinin constructs (Act-EF34 and Act-EF1234) containing two and four EF-hand motifs, respectively, were produced, and their folding properties were examined. Complex formation of Act-EF34 and Act-EF1234 with single- and double-Z-repeat constructs was studied. Act-EF34 was shown quantitatively to be necessary and sufficient for binding to Z-repeats, excluding the presence of additional high-affinity binding sites in the remaining part of the domain. The binding affinities of the different Z-repeats for Act-EF34 range from micromolar to millimolar values. The strongest of these interactions are comparable to those observed in troponin C−troponin I complexes. The binding affinities for Act-EF34 are maximal for Zr1 and Zr7, the two highly homologous sequences present in all muscle isoforms. No cooperative or additional contributions to the interaction were observed for Z-repeat double constructs. These findings have direct relevance for evaluating current models of Z-disk assembly.

The giant modular protein titin is a major component of striated vertebrate muscle (*1*, *2*). Single titin molecules form a third type of filament which starts at the Z-disk, where the N-terminus of titin is located (*3*, *4*), and extends up to the center of the sarcomere in the M-line, thus anchoring both ends of the molecule to the muscle fiber (Figure 1a). Titin is thought to play an important role in muscle assembly and ultrastructure (for reviews, see refs *3* and *5*−*9*). It is also implicated in muscle elasticity by conferring passive resistance of the sarcomere to stretching (*1*, *10*). To fulfill its structural role, titin interacts with several other muscle proteins such as myosin, MyB-C, and the M-protein (*11*). Recently, an interaction between titin and α-actinin was detected by two-hybrid screen methods (*12*, *13*). A repeated sequence motif of titin that is 45 residues long (Z-repeats), characterized by a relatively hydrophobic stretch, was shown to bind the C-terminus of α-actinin. Z-Repeats are localized in the sarcomere Z-disk near the N-terminus of titin (*14*) (Figure 1b). In humans, the number of Z-repeats varies in differentially spliced isoforms which are specific for different tissues (*14*). Zr1−Zr3 and Zr7 are present in all human titins, whereas Zr4−Zr6 are differentially expressed in skeletal muscles. All seven copies of Z-repeats are found in rabbit heart; chick heart muscles contain six repeats (*15*), while in chicken breast muscle, only the two flanking repeats (Zr1 and Zr7) are expressed (*16*). Differences in the number of Z-repeats are thought to account for variations in Z-band thickness (*13*, *14*, *17*).

α-Actinin is also a modular protein (Figure 1c). Its C-terminus contains a four-EF-hand motif, of which two are clearly identifiable from sequence analysis while the other two are hidden as described recently (*18*, *19*). The presence of this four-EF-hand calmodulin-like motif in the C-terminus of α-actinin had been originally suggested on the basis of homology with α-spectrin, a protein with a very similar architecture (*20*). All four EF-hands seem to have diverged to the point of losing their calcium binding ability (*21*). Further mapping of the titin−α-actinin interaction surface indicated that their recognition involves the C-terminal half of the calmodulin-like domain (*12*, *13*, *22*) and a 21-amino acid N-terminal region of the Z-repeats which becomes structured in a helical conformation upon binding (*19*). An additional binding site was described involving the region of titin directly adjacent to the last Z-repeat and the two central spectrin repeats of α-actinin (*4*). A model of Z-disk

* To whom correspondence should be addressed.
[‡] NIMR.
[§] EMBL.
[||] University College London.
[⊥] University of Ioannina.
[#] Universität Tübingen.
[@] Present address: IBMC, CNRS UPR 9021, 67084 Strasbourg, France.

10.1021/bi002739r CCC: $20.00
Published on Web 03/27/2001

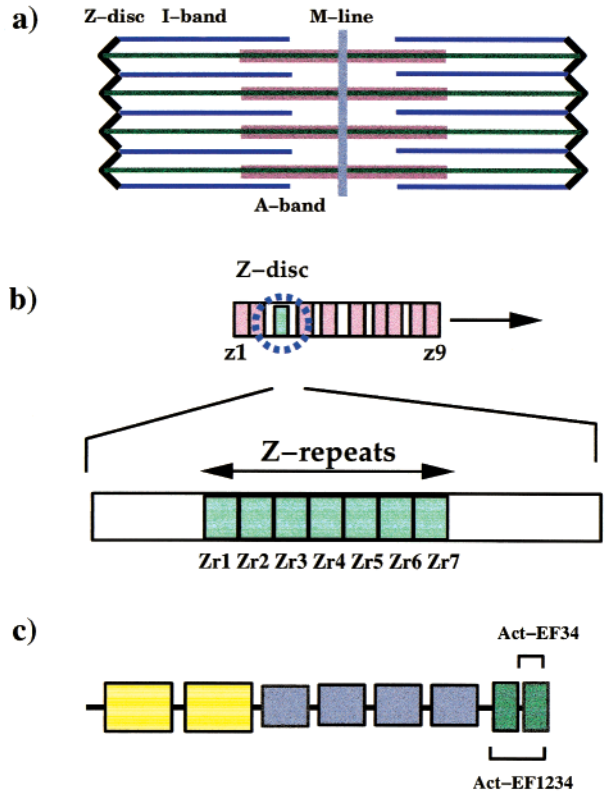

FIGURE 1: (a) Titin localization in the sarcomere. The green filament connecting the Z-disk to the M-line represents titin. Myosin and actin are represented in magenta and blue, respectively. The different regions of the sarcomere are explicitly indicated. (b) The modular structure of the N-terminus of titin. Pink and light green boxes are used for immunoglobulin domains and Z-repeats, respectively. (c) The modular structure of α-actinin. Yellow, blue, and dark green boxes are used for the calponin homology domains, spectrin-like repeats, and the constructs mentioned in the text, respectively.

assembly has been proposed on the basis of these interactions (*4*).

Interactions between titin and α-actinin may have great relevance in vivo since α-actinin, the major component of the Z-disk, is thought to anchor titin to the edge of the sarcomere and determine the assembly of the Z-disk (*23*, *24*). Interestingly, titin is indeed known to colocalize with α-actinin also during myofibrillogenesis (*25*−*27*). However, despite its importance for Z-disk ultrastructure and for our understanding of muscle assembly, a quantitative description of the interactions of Z-repeats with α-actinin and a comparison of the binding affinities is still lacking. It is, for instance, unclear whether all or only some Z-repeats are able to bind α-actinin with appreciable affinity. While initially only Zr7[1] was reported to interact with the C-terminal α-actinin domain, interactions with Zr1 and Zr2 have been described since for cell extracts (*3*, *13*). It is also not known if the interaction of the minimal binding units is modulated by the flanking regions.

In this study, we describe a structural characterization of the interactions between purified recombinant fragments spanning the sequences of the Z-repeats and of the C-terminus of α-actinin. We address specifically the question of whether the binding affinities of different Z-repeats are all comparable and what they are. We also study the influence that different choices of the domain boundaries of the α-actinin C-terminus and of the Z-repeats have on their structures and on their binding properties. A combination of circular dichroism (CD) and nuclear magnetic resonance (NMR) spectroscopies as well as isothermal titration calorimetry (ITC) has been used to provide a consistent and complementary description of the binding of the titin Z-repeats to α-actinin. It is hoped that our results may have a direct influence on current models of Z-disk assembly.

MATERIALS AND METHODS

Sample Production. The sequences of the peptides used for this study are summarized in Figure 2. Initially, Z-repeat samples were produced synthetically by standard solid-phase methods (*28*). The N- and C-termini were both unprotected. Peptide purity (95%) was determined by HPLC, and composition was confirmed by mass spectrometry. Later, when an efficient method for the production of recombinant peptides as fusion proteins was set up, the peptides were expressed in *Escherichia coli*. Results for the same peptide from the two sources are entirely compatible. Titin constructs were amplified either from total rabbit cardiac cDNA or from a human skeletal muscle cDNA library (Clontech). The α-actinin constructs were produced by amplification of the human skeletal muscle α-actinin 2 sequence (EMBL/GenBank, accession no. M86406); one construct contains the whole C-terminal region of α-actinin from residues 745 to 894 (Act-EF1234), and the other contains the last 72 C-terminal amino acids (Act-EF34). PCR amplification was performed following the method described in ref *13*. The restriction sites for enzymes *Nco*I and *Kpn*I (Boheringer) were included at the N- and C-termini of the fragments to facilitate subcloning into a modified pET vector. The *Nco*I restriction site added an extra methionine to the N-terminus of the peptides. All α-actinin and single-Z-repeat constructs were produced as follows: a six-His tag, the *S. Japonicum* glutathione transferase (GST), and a seven-amino acid recognition site for recombinant tobacco endovirus (rTEV) protease followed by the heterologous peptide. The TEV cleavage site results in two additional residues (Gly-Ala) on the N-terminus of the construct, prior to the methionine. The double-Z-repeat constructs were produced only with the six-His tag at their N-termini. The expression of soluble His-tagged proteins was induced in the *E. coli* BL21[DE3]pLysS strain using 0.5 mM isopropyl β-D-thiogalactopyranoside (IPTG), when the absorbance at 595 nm was 0.5.

Protein Purification. The first purification step was carried out on a Ni−NTA agarose column (QIAGEN). Cleavage of the fusion GST was achieved overnight at room temperature using GIBCOBRL TEV recombinant protease (catalog no. 10127-017). Separation of the GST from the peptides was performed by gel filtration in Pharmacia Superdex75 16/60 using as a buffer 20 mM Tris-HCl (pH 8.0), 200 mM NaCl, and 2 mM β-mercaptoethanol. Samples were desalted on a Sephadex G-25M PD-10 column against 20 mM sodium phosphate buffer (pH 6.6) and 10 mM NaCl. Sample concentrations were determined by UV (the extinction

[1] Abbreviations: CD, circular dichroism; GFP, green fluorescent protein; NMR, nuclear magnetic resonance; 1D and 2D, one- and two-dimensional, respectively; PCR, polymerase chain reaction; Z*rn*, *n*th Z-disk repeat; ITC, isothermal titration calorimetry; TnC, troponin C; TnI, troponin I.

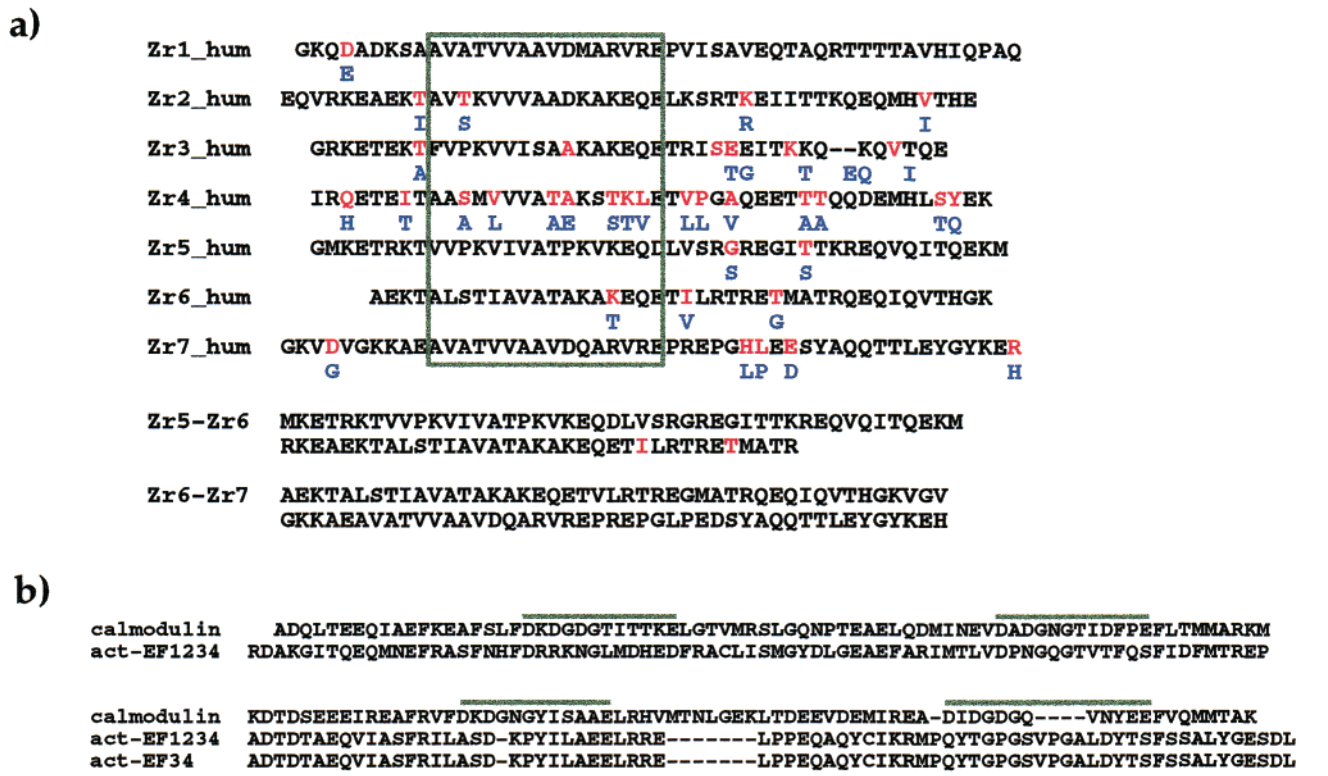

FIGURE 2: (a) Alignment of the human Z-repeat sequences. All repeats except for Zr4 were produced for this study. Zr4 is the most divergent of the Z-repeats among species and, together with Zr5, is often differentially spliced out. For historical reasons, the rabbit sequences were used. They are more than 90% homologous with their human orthologues (the differences between human and rabbit are indicated with blue letters under the corresponding positions marked in red). For most of the repeats, the differences occur outside the interacting region [here marked with a green square (*18*, *19*)]. The rabbit and human sequences of Zr2 differ by three amino acids in the N-terminus, so the human sequence was cloned for this repeat and used in this study. (b) Comparison of the sequences of the Act-EF1234 and Act-EF34 constructs with that of calmodulin. The positions of the calcium-binding loops in calmodulin are shown with green lines.

coefficients at 280 nm of Act-EF34 and Act-EF1234 are 6520 and 7920 M^{-1} cm^{-1}, respectively) or by amino acid analysis for the peptides without chromophores. At least two independent amino acid analysis measurements were taken for each set of titrations. The mass was determined to be correct by electrospray mass spectrometry.

CD Measurements. CD spectra were recorded on a Jasco J-715 CD spectropolarimeter, fitted with a thermostated cell holder, and interfaced to a Neslab water bath. The instrument was calibrated with a 0.10% aqueous solution of *d*-10-camphorsulfonic acid (d10-CSA, Aldrich). Quartz cuvettes (Hellma) with path lengths ranging from 2 to 10 mm were used, depending on the sample concentration. Typically, spectra were recorded in 20 mM sodium phosphate buffer, containing 2 mM β-mercaptoethanol, at pH 6.6 and 20 °C and were baseline corrected by subtraction of the appropriate buffer spectrum. The combined absorbance of the cell, sample, and solvent was kept to less than 1 over the measured spectral range (between 201 and 260 nm). The spectra were averaged over five scans. Titration curves with α-actinin concentrations ranging from 2 to 40 μM were recorded, in which the protein concentration was kept constant and increasing amounts of the titin peptide were added. A "reverse" titration was also performed, maintaining the titin concentration at 10 μM. Ellipticity variations had their maximal value at 222 nm, but were also monitored at 228 nm where the absorbance of the solutions was lower. Each titration was repeated at least twice at different concentrations.

Number of Residues in an α-Helical Conformation. CD intensities were calculated using the molar concentration of peptide or protein ($\Delta\epsilon_M$) rather than on a per residue basis ($\Delta\epsilon_{MRW} = \Delta\epsilon_{M/N_{res}}$) to facilitate direct comparison of the different components (free and complexed species) which involve different numbers of residues, N_{res}. The measurements of $\Delta\Delta\epsilon_M$ at 222 nm (calculated as $\Delta\epsilon_M$ for the protein−peptide complex minus $\Delta\epsilon_M$ for the free protein) were used to estimate the number of peptide residues adopting a helical conformation in the complex (N_H) using the formula

$$N_H = [\Delta\Delta\epsilon_M(222\text{ nm}) - 0.194N]/[\Delta\epsilon_{MRW}(222\text{ nm}) - 0.194]$$

where $\Delta\epsilon_{MRW}(222\text{ nm}) = [12.122(1 - 2.5/N)]$ is the signal expected for a completely helical peptide with N peptide bonds (*29*).

Calorimetry. Experiments were carried out at 25 °C using an MCS isothermal titration calorimeter (MicroCal Inc., Northampton, MA). Titrations were performed as described elsewhere (*30*, *31*). All protein samples were exhaustively dialyzed against 20 mM sodium phosphate, 5 mM EDTA, and 2 mM dithiothreitol (pH 6.6). In a typical experiment, 18 aliquots (15 μL) of one component (50 μM) were injected into the other (10 μM) in the ITC cell. The heats of dilution of ligand into the buffer were determined separately and subtracted from the titration prior to analysis. The titration

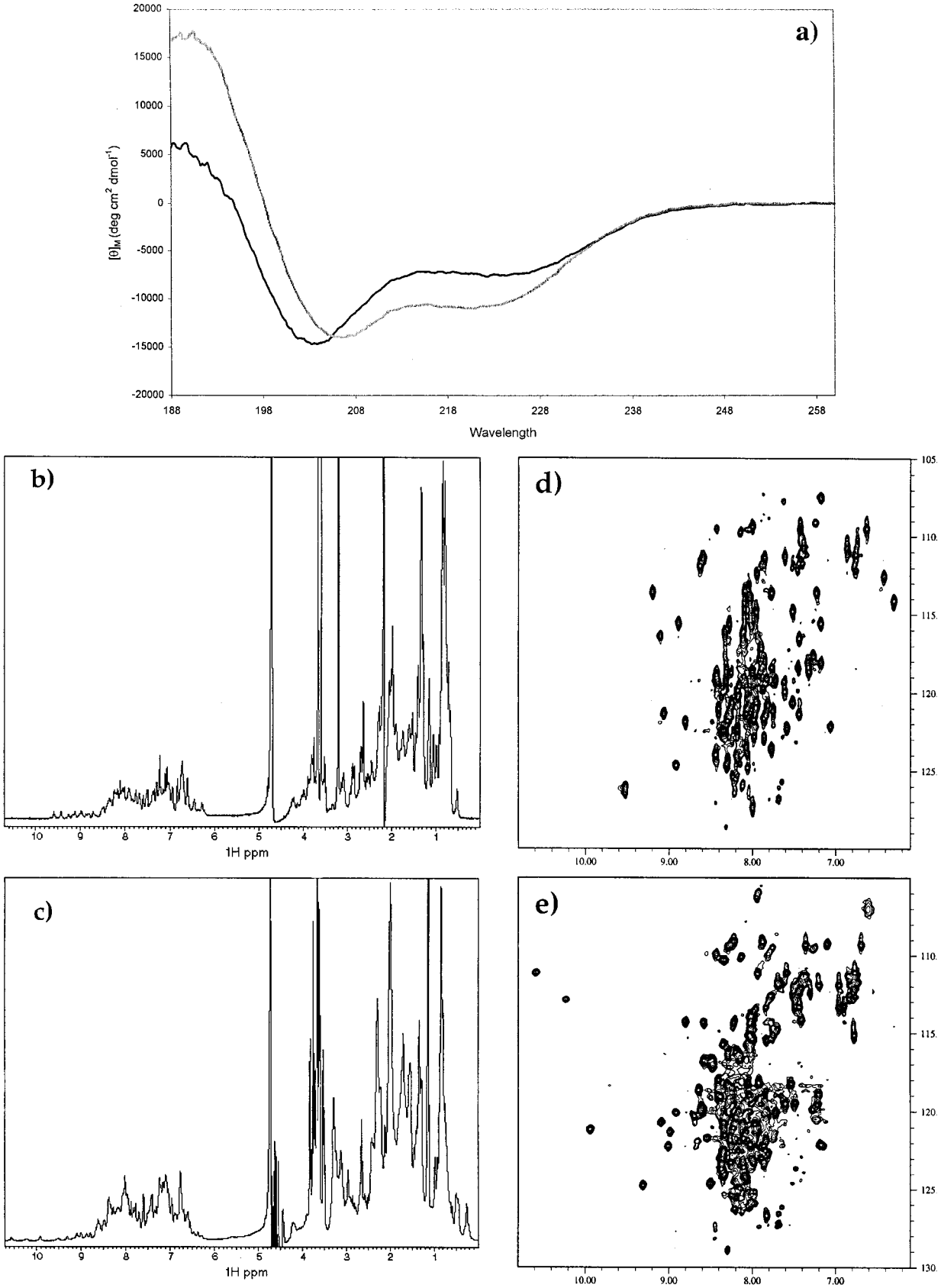

FIGURE 3: (a) Far-UV CD spectra of Act-EF34 (black) and Act-EF1234 (gray). (b and c) ^{1}H 1D spectra of Act-EF34 and Act-EF1234 recorded at 600 MHz and 27 °C. (d and e) $^{1}H-^{15}N$ HSQC spectra of Act-EF34 and Act-EF1234. The spectra do not show additivity, as discussed in the text.

data were fit using the Origin software supplied with the calorimeter to a single-site model with three floating variables, stoichiometry (N), binding constant (K_b), and the enthalpy of interaction (ΔH) (*31*). The entropy and free energy changes for binding can be calculated from the equations $\Delta G = \Delta H - T\Delta S$ and $\Delta G^\circ = RT \ln K_d$. At least

three independent data sets were collected for each measurement and averaged.

NMR Experiments. The NMR spectra were acquired on a Varian Unity 600 MHz instrument at 27 °C, as described by Atkinson et al. (*18*, *19*). Water suppression was achieved by the WATERGATE pulse sequence. Samples were ~0.7 mM in 20 mM sodium phosphate buffer at pH 6.6. NMR data were processed using the NMRPipe software (32) running on an SGI O2 workstation. Full assignment and secondary structure determination of the Act-EF34−Zr7 complex is described by Atkinson et al. (*18*, *19*).

RESULTS

Act-EF34 and Act-EF1234 Are Independently Folded Proteins, but the Structure of Uncomplexed Act-EF34 Is Modulated by the Presence of the Flanking Domain. The folds of the two uncomplexed Act-EF34 and Act-EF1234 constructs were probed by CD and NMR and compared. The far-UV CD spectra of both constructs are typical of folded α-helical proteins with minima at 208 and 222 nm (Figure 3a). The helical content corresponds to 32 and 37% for Act-EF34 and Act-EF1234, respectively.

One-dimensional ^{1}H NMR spectra of the constructs confirm that both proteins are folded in solution and nonaggregated; the resonances are well-dispersed with relatively narrow line widths (Figure 3b,c). The presence of upfield resonances in the range of 0−0.7 ppm is also typical of folded proteins arising from aliphatic protons in persistent proximity to aromatic groups. The HSQC spectrum of Act-EF1234, however, is not simply that of Act-EF34 plus additional peaks from the 70 N-terminal amino acids (Figure 3d,e). The spectrum of Act-EF34 contains more peaks than what is expected from its sequence, but none of them seems to have a corresponding peak in the spectrum of Act-1234, even when contouring at levels close to the noise. However, the degree of purity as assessed by both gel filtration and mass spectrometry excludes the possibility of contaminants or degradation products. This implies that the last 70 amino acids of α-actinin adopt more than one conformation and that their behavior is strongly influenced by the choice of the construct. The N-terminal portion of the uncomplexed Act-EF1234 must therefore have an influence on the structure of its C-terminal portion.

No effect of calcium titration on the spectra was observed.

The Z-Repeats Bind to Act-EF34 with Different Affinities and Gain Secondary Structure. Changes in the conformation of α-actinin upon binding to the titin peptides were monitored by far-UV circular dichroism. CD spectra of peptides in this range reflect the conformation of the backbone. The far-UV CD spectra of the free Z-repeat peptides in aqueous solution are typical of random coil peptides (*18*, *19*). Changes in the helical signal can therefore be attributed to complex formation. The peptides exhibit three different types of behavior. (i) Titration of Act-EF34 with Zr1 or Zr7 results in a comparable gain in helical signal, which is well above the noise and clearly due to complex formation (Figure 4). For these peptides, the titration curves provide clear evidence for a 1:1 stoichiometry of binding, in the range of concentrations that have been studied (Figure 5). (ii) Titration of Act-EF34 with Zr2, Zr5, and Zr6 leads to a small gain of helical signal that cannot be attributed clearly to complex formation.

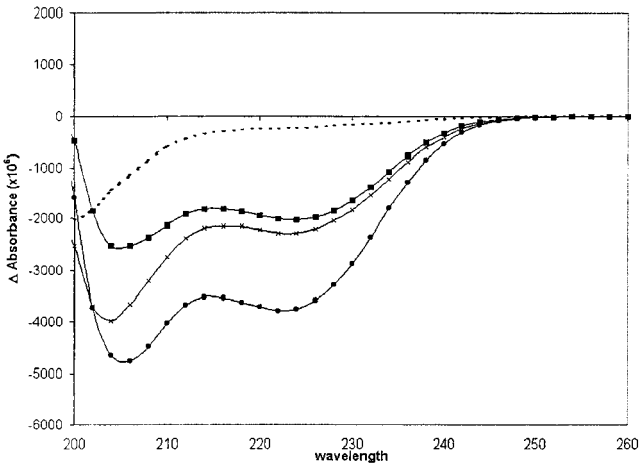

FIGURE 4: Gain of signal for the Act-EF34−Zr7 complex recorded by far-UV CD spectroscopy. The concentration of each component was 40 μM, and the path length was 2 mm. The spectra of the isolated components, Zr7 (•••), Act-EF34 (■), and the complex (●), are shown. The sum of the spectra of the two isolated components is also reported for comparison (×).

(iii) Titration of Act-EF34 with Zr3 results in a gain of helical signal intermediate between that obtained for Zr1 and Zr7 and for Zr2, Zr5, and Zr6. A comparison of the titration curves for Zr1, Zr3, and Zr7 is shown in Figure 5. If it is assumed that the changes in the far-UV CD spectra may be solely attributed to the increased helicity of the Z-repeat peptides in the complexes, the number of residues in Zr1 and Zr7 adopting an α-helical conformation upon complex formation ranges from 18 to 21, in good agreement with NMR studies (*18*, *19*). Upon complex formation with Zr7, the melting point increases from 42 to >50 °C. The affinities (as estimated by curve fitting) of the Act-EF34−single repeat complexes differ and are greatest for Zr1 and Zr7.

Quantification of the Act-EF34−Zr7 and Act-EF1234−Zr7 Affinities. ITC was used to quantify the binding affinity of the Act-EF34−Zr7 and Act-EF1234−Zr7 complexes. The complex of Zr7 with Act-EF34 was formed by performing the titrations in both directions, that is, by injecting Zr7 into Act-EF34 and vice versa. Both titrations gave identical results within experimental error (Figure 6 and Table 2). These results support the validity of a single-binding mode model and prove that the binding is not coupled to additional equilibria. The titrations of Zr7 with both Act-EF1234 and Act-EF34 exhibited stoichiometries close to 1, indicating 1:1 binding events with affinities comparable within experimental error (K_d values given in Table 2). The thermodynamics of the interaction display similar characteristics and are enthalpically driven and entropically disfavored. There is no evidence for any additional high-affinity sites on Act-EF1234.

The titration isotherms for the interaction of Zr2 and Zr3 with Act-EF34, under conditions and concentration regimes similar to those employed for Zr7, showed that the interaction was too weak to be detected, in agreement with the CD measurements. For these and other low-affinity complexes, the values obtained by CD were taken to be indicative of the relative strength of the interactions.

Act-EF34 Is the Unit Necessary and Sufficient for the Interaction. The complexes of Act-EF34 and Act-EF1234 with Zr7 were further characterized by NMR. Complexes

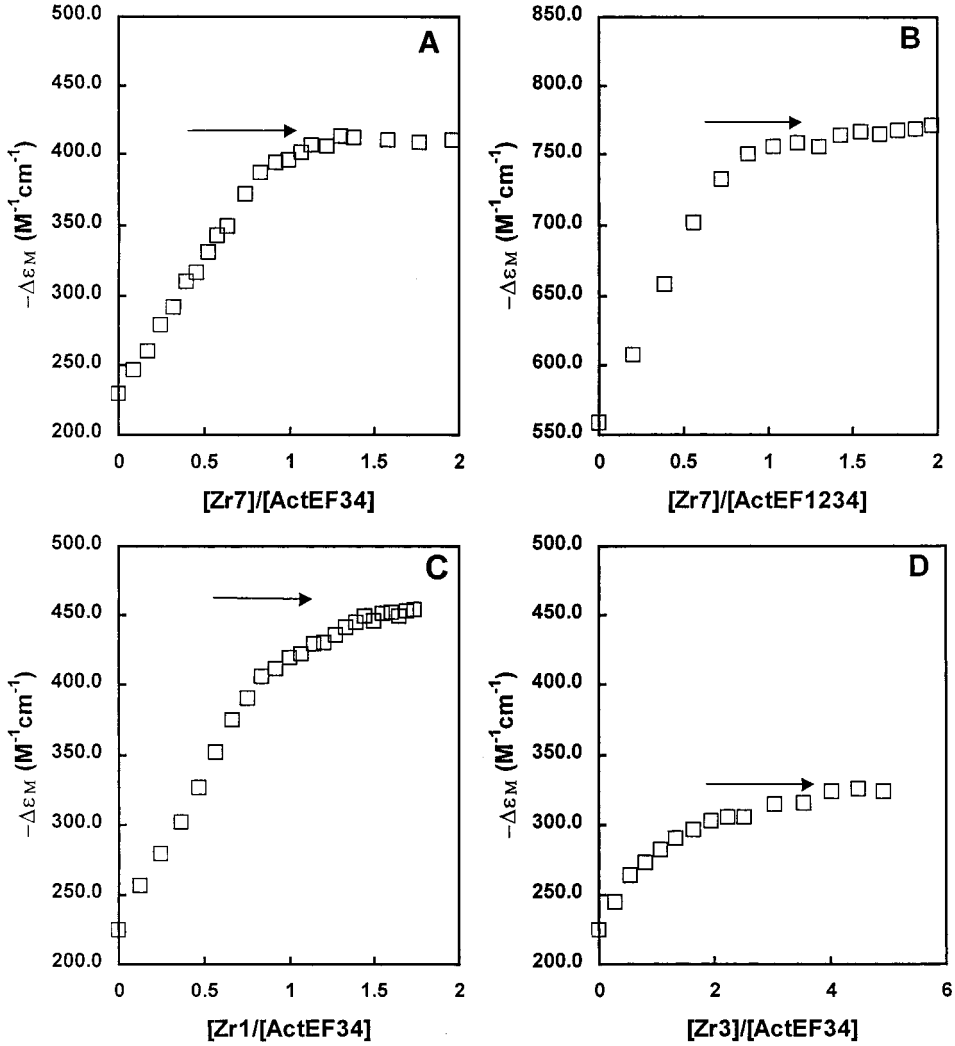

FIGURE 5: Titration curves of Act-EF34 and Act-EF1234 with the Zr1, Zr3, and Zr7 peptides. An arrow indicates the plateau obtained from fitting.

were formed either by titrating the ^{15}N-labeled α-actinin constructs with unlabeled peptide or by mixing the two components prior to purification [as described by Atkinson et al. (*18, 19*)]. Two-dimensional ^{1}H−^{15}N HSQC spectra show that, upon complex formation, the spectrum of Act-EF34 changes drastically, while the positions of most of the most dispersed peaks of Act-EF1234 remain unaltered (Figure 7). The number of resonances in the spectrum of the complexed Act-EF34 decreases to what is expected for this construct. Full assignment of this spectrum proves conclusively that complexed Act-EF34 adopts a unique conformation (*18, 19*). Act-EF34 clearly undergoes a major conformational change on binding to Zr7. Unlike those of the uncomplexed proteins, the spectra of the complexed proteins are mostly additive; i.e., resonances of Act-EF34 in the complex are found at identical positions in the spectrum of Act-EF1234 in its complex with Zr7. Thus, Act-EF34 binds in the same manner to Zr7 whether it is isolated or in the context of Act-EF1234. The remaining resonances may be attributed to the N-terminal portion of Act-EF1234 and include the most downfield shifted amide resonances. Interestingly, many of the resonances attributed to the N-terminal portion of Act-EF1234 are found in the spectrum of uncomplexed Act-EF1234, indicating that its conformation is largely insensitive to whether the C-terminal portion is bound to Zr7. This implies that, while the conformations of the uncomplexed domains are different, the structures of the final complexes are comparable and the presence of the peptide locks the proteins into one conformation. These results further support the view that the Act-EF34−Zr7 complex is the minimal unit necessary and sufficient for the interaction. The complex can therefore be taken as a working model for understanding the interactions between α-actinin and titin Z-repeats.

Constructs Containing Two Z-Repeats in Tandem Have Affinities Comparable to Those of Single Z-Repeats. The possible influence on the affinities of the presence of more than one tandem repeat and/or of the choice of domain boundaries for the Z-repeats was checked by studying the behavior of Zr5−Zr6 and Zr6−Zr7 double constructs. The helical signals developed in far-UV CD spectra by the Act-EF34−Zr6−Zr7 and Act-EF1234−Zr7 complexes correspond to $\Delta\Delta\epsilon_M$ values of 207 and 200 cm^{-1} M^{-1}. These numbers are directly comparable to the value observed for the Act-EF34−Zr7 complex ($\Delta\Delta\epsilon_M = 210$ cm^{-1} M^{-1}, spectra not shown), thus suggesting that the contribution of Zr6 to the complex is negligible. Formation of a Act-EF34−Zr5−Zr6 complex leads to some increase in the CD helical signal, but it remains lower than that of the Act-EF34−Zr3 complex, suggesting that the presence of two repeats promotes only

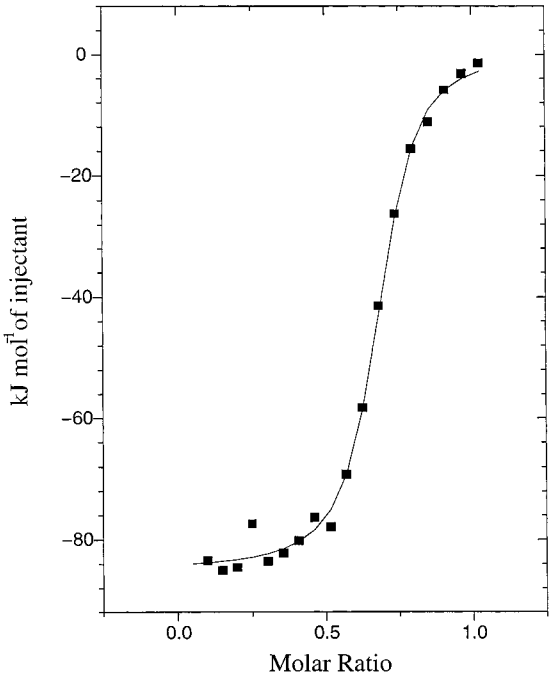

FIGURE 6: ITC binding isotherm obtained for the interaction of Zr7 with Act-EF34. Eighteen 15 μL aliquots of Zr7 (50 μM) were injected into the calorimeter cell containing Act-EF34 (10 μM) at 25 °C.

Table 1: Summary of the Affinities Estimated by CD[a]

	$\Delta\epsilon_M$(222 nm) (M^{-1} cm^{-1})[b]	$\Delta\Delta\epsilon_M$(222 nm) (M^{-1} cm^{-1})[c]	N_H[d]	N_H[e]	K_d (nM)[f]
Act-EF34	230	−	23	−	−
Act-EF1234	560	−	56	−	−
Act-EF34−Zr1	455	225	−	23	200−300
Act-EF34−Zr3	345	115	−	12	>4000
Act-EF34−Zr7	425	195	−	20	100−250
Act-EF1234−Zr7	770	210	−	22	100−300

[a] The spectra were recorded in 20 mM sodium phosphate containing 2 mM β-mercaptoethanol at pH 6.6 and 20 °C. [b] Molar CD extinction coefficients. [c] Calculated as the difference of $\Delta\epsilon_M$(222 nm) for the complex and for the protein alone. It represents the acquisition of signal due to complex formation. [d] Total number of residues in a helical conformation in the α-actinin constructs. [e] Total number of residues in a helical conformation in the bound Z-repeats. [f] Results obtained as the average of at least two independent measurements.

Table 2: Thermodynamic Parameters for the Binding of Zr7 to Act-EF1234 and Act-EF34[a]

complex	K_b ($\times 10^{-6}$ M^{-1})[b]	K_d (nM)[c]	ΔH (kJ mol^{-1})
Act-EF34−Zr7	8.19 (3.12)	120	−63.8
Act-EF1234−Zr7	10.32 (3.55)	100	−79.1

[a] The standard deviations for a set of three independent measurements are given in parentheses. [b] Binding constants. [c] Rounded reciprocals of K_b values.

some very weak binding which could not be observed for the single-repeat constructs.

DISCUSSION

The goal of this project was to study the protein−protein interactions taking place in the Z-disk between α-actinin and titin by biophysical methods, with a view of gaining new insights into Z-disk assembly. A combination of CD, ITC, and NMR methods was applied to monitor the thermodynamics as well as the stoichiometry of the complexes and to dissect the interactions into their minimal components. In doing so, we have compared the fold of two constructs which contain two and four EF-hand motifs, respectively. The presence of a calmodulin-like domain has been experimentally verified for α-spectrin, a protein which shares with α-actinin the same architecture and a high degree of sequence homology (*20*). We have previously shown conclusively that Act-EF34 contains two EF-hands (*18*, *19*). We demonstrate here that Act-EF1234 also folds as a stable domain with a high predominance of helical conformation as expected if formed from two similar subunits. Its helical content is comparable to that observed for calcium-loaded calmodulin (30−45%; *33*) and slightly lower than that described for the C-terminal domain of α-spectrin (*20*). No calcium dependence was observed as expected from the significant divergence of the putative calcium-binding loops from the classical

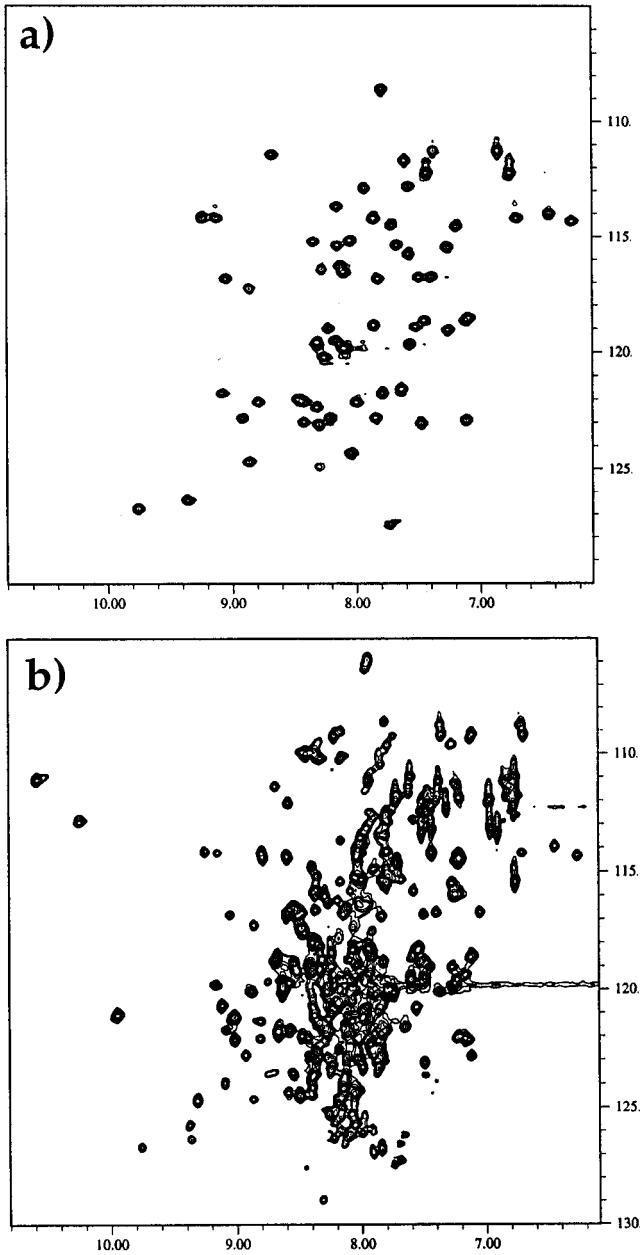

FIGURE 7: $^1H-^{15}N$ HSQC spectra of (a) ^{15}N-labeled Act-EF34−unlabeled Zr7 and (b) ^{15}N-labeled Act-EF1234−unlabeled Zr7 complexes.

EF-hand hallmark, having insertions and/or deletions and mutations in the calcium-binding motifs. One feature was however interesting because it was unexpected. Additivity of the NMR spectra of component domains is a characteristic feature of calmodulin-like proteins; the spectrum of the whole molecule is almost the exact superposition of the spectra of the N- and C-terminal subdomains (*20*, *34*, *35*). In calmodulin-like proteins, this behavior is attributed to the independence of the two globular domains arising from the flexible nature of the linker between them. The spectra of uncomplexed Act-EF34 and Act-EF1234 do not exhibit additivity; that is, the spectrum of Act-EF1234 is not the sum of resonances at the same frequencies from the spectrum of Act-EF34 and additional resonances from the N-terminal domain (Figure 3d,e). This suggests that, although both α-actinin constructs are folded, the conformations of the two halves of Act-EF1234 are not as independent as in calmodulin or that, in the absence of a ligand, Act-EF34 adopts a conformation different from that of the same sequence in Act-EF1234. A major conformational rearrangement is observed upon complexation which locks the structures of the complexes into a similar and unique conformation (Figure 7).

Further, we examined the thermodynamics of complex formation of titin Z-repeats and α-actinin EF-domains using CD and ITC techniques. Both techniques have an advantage in that no labeling, tagging, or other modification of the reactants is necessary. CD allowed a screening of the conditions and of the relative affinities even for very weak complexes, allowing a direct estimate of the coil-to-helix transitions observed for the peptides upon binding to the EF-hand constructs. ITC is now a well-established method for the measurement of the stoichiometry, dissociation constants (K_d), and enthalpy change, ΔH, of a binding process. It was used to obtain a more quantitative measure of the affinities of the strongest complexes.

The binding affinity of the Act-EF34−Zr7 complex is comparable to that of the Act-EF1234−Zr7 complex, so we may conclude that the N-terminal region of Act-EF1234 does not contribute significantly to the binding, in agreement with previous qualitative studies (*13*, *22*). It is therefore expected that the complex will be different from that formed by calmodulin and most of its peptide targets (for a review, see ref *36*). The affinities of the Act-EF34−Z-repeat complexes differ and range from millimolar to nanomolar values. Zr1 and Zr7 have comparable values and the highest affinities, consistent with the fact that the interacting region is located near the N-terminus of the repeats (*18*, *19*) where Zr1 and Zr7 have the highest degree of homology. Zr2, Zr5, and Zr6 have very weak binding (in the millimolar range), while Zr3 shows intermediate affinity. No appreciable effect of the choice of the peptide sequence boundaries was observed. Although weaker than the binding of calmodulin with some of its partner peptides, the binding observed for Zr1 and Zr7 is comparable to that between the calcium-loaded C-terminal domain of TnC and two TnI peptides (*37*). This is interesting in light of the proposed mode of binding between Zr7 and Act-EF34; a growing body of experimental evidence suggests that the manner of binding of Zr7 in the Act-EF34−Zr7 complex could be similar to that of the TnC−TnI(1−47) complex (*18*, *19*, *38*). Our data should also be compared with the results published by Ayoob et al. (*15*). In that study, different isolated Z-repeats have different Z-disk localization behavior when introduced by transfection into embryonic chick cardiac cells. The results reported in this paper broadly correlate with their data, suggesting that higher affinities of the α-actinin−Z-repeat complexes result in more efficient localization. However, a precise correlation at the level of single repeats might be difficult because localization efficiency is strongly influenced by the presence and the length of appropriate linkers between GFP and the Z-repeat constructs (15).

The prominent role of Zr1 and Zr7 supports the observation that nearly all titin Z-repeats can be differentially spliced in different muscles except for the flanking Zr1 and Zr7, suggesting that these two repeats form a distinct essential subgroup (*3*, *14*, *16*). Adjacent Z-disk fragments have been shown to have different effects on myofibrillogenesis. However, we cannot at this stage exclude the possibility that even the much weaker interactions between the other Z-repeats and α-actinin might play some role in vivo; in the context of the Z-disk, the affinities of individual repeats might be cooperatively enhanced both by the presence of several anchoring points and by the fixed location of the titin filament. On the other hand, the interaction of α-actinin with Z-repeats is only one of several reported interactions. The C-terminus of α-actinin has also been implicated in interactions with the protein ZASP (*39*, *40*), posing the question of whether these complexes can be formed at the same time. The weak α-actinin−titin interactions might therefore be "designed" to be conveniently replaced by stronger ones at some stage of myofibrillogenesis. Clearly, much more work is needed to gain a detailed description of the complex network of molecular complexes implicated in the assembly of the Z-disk.

ACKNOWLEDGMENT

We thank Drs. Mathias Gautel and Uwe Sauer for helpful discussion, Dr. David J. Thomas for help in manuscript preparation, and Prof. Günther Jung for providing the facilities for peptide synthesis. A.B. was the recipient of a postdoctoral fellowship from the von Humboldt Foundation.

REFERENCES

1. Maruyama, K., Matsubara, S., Nonomura, Y., Kimura, S., Ohashi, K., Murakami, F., Handa, S., and Eguchi, G. (1977) Connectin, an elastic protein of muscle: characterization and function, *J. Biochem. 82*, 317−337.
2. Wang, K., McClure, J., and Tu, A. (1979) Titin: major myofibrillar components of striated muscle, *Proc. Natl. Acad. Sci. U.S.A. 76*, 3698−3702.
3. Gregorio, C. C., Granzier, H., Sorimachi, H., and Labeit, S. (1999) Muscle assembly: a titanic achievement? *Curr. Opin. Cell Biol. 11*, 18−25.
4. Young, P., Ferguson, C., Bauelos, S., and Gautel, M. (1998) Molecular structure of the sarcomeric Z-disk: two types of titin interactions lead to an asymmetrical sorting of α-actinin, *EMBO J. 17*, 1614−1624.
5. Maruyama, K. (1994) Connectin, an elastic protein of striated muscle, *Biophys. Chem. 50*, 73−85.
6. Trinick, J. (1994) Titin and nebulin: protein rulers in muscle, *Trends Biochem. Sci. 19*, 405−409.
7. Keller, T. C. S., III (1995) Structure and function of titin and nebulin, *Curr. Opin. Cell Biol. 7*, 32−38.

8. Trinick, J. (1996) Titin as a scaffold and spring, *Curr. Biol. 6*, 258−260.
9. Maruyama, K. (1997) Connectin/titin, giant elastic protein of muscle, *FASEB J. 11*, 341−345.
10. Horowits, R., Maruyama, K., and Podolsky, R. J. (1989) Elastic behavior of connectin filaments during thick filament movement in activated skeletal muscle, *J. Cell Biol. 109*, 2169−2176.
11. Soteriou, A., Gamage, M., and Trinick, J. (1993) A survey of interactions made by the giant protein titin, *J. Cell Sci. 104*, 119−123.
12. Ohtsuka, H., Yajima, H., Maruyama, K., and Kimura, S. (1997) Binding of the N-terminal 63 kDa portion of connectin/titin to α-actinin as revealed by the yeast two-hybrid system, *FEBS Lett. 401*, 65−67.
13. Sorimachi, H., Freiburg, A., Kolmerer, B., Ishiura, S., Stier, G., Gregorio, C. C., Labeit, D., Linke, W. A., Suzuki, K., and Labeit, S. (1997) Tissue-specific expression and α-actinin binding properties of the Z-disk titin: implications for the nature of vertebrate Z-disks, *J. Mol. Biol. 270*, 688−695.
14. Gautel, M., Goulding, D., Bullard, B., Weber, K., and Fürst, D. O. (1996) The central Z-disk region of titin is assembled from a novel repeat in variable copy numbers, *J. Cell Sci. 109*, 2747−2754.
15. Ayoob, J. C., Turnacioglu, K. K., Mittal, B., Sanger, J. M., and Sanger, J. W. (2000) Targeting of cardiac muscle titin fragments to the Z-bands and dense bodies of living muscle and non-muscle cells, *Cell Motil. Cytoskeleton 45*, 67−82.
16. Peckham, M., Young, P., and Gautel, M. (1997) Constitutive and variable regions of Z-disk titin/connectin in myofibril formation: a dominant-negative screen. *Cell. Struct. Funct. 22* (1), 95−101.
17. Luther, P. K. (2000) Three-dimensional structure of a vertebrate muscle Z-band: Implications for titin and α-actinin binding, *J. Struct. Biol. 129*, 1−16.
18. Atkinson, R. A., Joseph, C., Kelly, G., Muskett, F. W., Frenkiel, T. A., and Pastore, A. (2000) Assignment of the ^{1}H, ^{13}C and ^{15}N resonances of the C-terminal EF-hands of α-actinin, in a 14 kDa complex with Z-repeat 7 of titin, *J. Biomol. NMR 16*, 277−278.
19. Atkinson, R. A., Joseph, C., Dal Piaz, F., Birolo, L., Stier, G., Pucci, P., and Pastore, A. (2000) The binding of α-actinin to titin: implications for Z-disk assembly, *Biochemistry 39*, 5255−5264.
20. Travé, G., Pastore, A., and Saraste, M. (1995) The C-terminal domain of α-spectrin is structurally related to calmodulin, *Eur. J. Biochem. 227*, 35−42.
21. Beggs, A. H., Byers, T. J., Knoll, J. H. M., Boyce, F. M., Bruns, G. A. P., and Kunkel, L. M. (1992) Cloning and characterization of two human skeletal muscle α-actinin genes located on chromosomes 1 and 11, *J. Biol. Chem. 267*, 9281−9288.
22. Ohtsuka, H., Yajima, H., Maruyama, K., and Kimura, S. (1997) The N-terminal Z repeat 5 of connectin/titin binds to the C-terminal region of α-actinin, *Biochem. Biophys. Res. Commun. 235*, 1−3.
23. Schulze, H., Huckriede, A., Noegel, A. A., Schleicher, M., and Jockusch, B. M. (1989) α-Actinin synthesis can be modulated by antisense probes and is autoregulated in non-muscle cells, *EMBO J. 8*, 3587−3593.
24. Pavalko, F. M., Schneider, G., Burridge, K., and Lim, S. S. (1995) Immunodetection of alpha-actinin in focal adhesions is limited by antibody inaccessibility. *Exp. Cell Res. 217* (2), 534−540.
25. Schultheiss, T., Lin, Z. X., Lu, M. H., Murray, J., Fischman, D. A., Weber, K., Masaki, T., Imamura, M., and Holtzer, H. (1990) Differential distribution of subsets of myofibrillar proteins in cardiac nonstriated and striated myofibrils. *J. Cell Biol. 110* (4), 1159−1172.
26. Rhee, D., Sanger, J. M., and Sanger, J. W. (1994) The premyofibril: evidence for its role in myofibrillogenesis. *Cell Motil. Cytoskeleton 28* (1), 1−24.
27. Turnacioglu, K. K., Mittal, B., Sanger, J. M., and Sanger, J. W. (1996) Partial characterization of zeugmatin indicates that it is part of the Z-band region of titin. *Cell Motil. Cytoskeleton 34* (2), 108−121.
28. Jung, G., and Beck-Sickinger, A. G. (1992) Multiple peptide synthesis methods and their applications, *Angew. Chem., Int. Ed. Engl. 31*, 367−383.
29. Scholtz, J. M., Qian, H., York, E. J., Stewart, J. M., and Baldwin, R. L. (1991) Parameters of helix-coil transition theory for alanine-based peptides of varying chain lengths in water. *Biopolymers 31*, 1463−1470.
30. Wiseman, T., Williston, S., Brandts, J. F., and Lin, L. N. (1989) Rapid measurement of binding constants and heats of binding using a new titration calorimeter, *Anal. Biochem. 179*, 131−137.
31. Ladbury, J. E., and Chowdhry, B. Z. (1996) Sensing the heat: the application of isothermal titration calorimetry to thermodynamic studies of biomolecular interactions, *Chem. Biol. 3*, 791−801.
32. Delaglio, F., Grzesiek, S., Vuister, G. W., Zhu, G., Pfeifer, J., and Bax, A. (1995) NMRPipe: a multidimensional spectral processing system based on UNIX pipes, *J. Biomol. NMR 6*, 277−293.
33. Klee, C. (1988) Interaction of calmodulin with Ca^{2+} and target proteins, in *Molecular aspects of cellular regulation, calmodulin* (Cohen, P., and Klee, C. B., Eds.) Vol. 5, pp 35−56, Elsevier, Amsterdam.
34. Aulabagh, A., Niemczura, W. P., and Gibbons, W. A. (1984) High-field proton NMR studies of tryptic fragments of calmodulin: a comparison to the native protein, *Biochem. Biophys. Res. Commun. 118*, 225−232.
35. Ikura, M., Minowa, O., Yazawa, M., Yagi, K., and Hikichi, K. (1987) Sequence-specific assignments of downfield-shifted amide proton resonances of calmodulin, *FEBS Lett. 219*, 17−21.
36. Zhang, M., and Yuan, T. (1998) Molecular mechanisms of calmodulin's functional versatility, *Biochem. Cell. Biol. 76*, 313−323.
37. Mercier, P., Li, M. X., and Sykes, B. D. (2000) Role of the structural domain of troponin C in muscle regulation: NMR studies of Ca^{2+} binding and subsequent interactions with regions 1−40 and 96−115 of troponin I, *Biochemistry 39*, 2902−2911.
38. Vassylyev, D. G., Takeda, S., Wakatsuki, S., Maeda, K., and Maeda, Y. (1998) Crystal structure of troponin C in complex with troponin I fragment at 2.3 Å resolution, *Proc. Natl. Acad. Sci. U.S.A. 95*, 4847−4852.
39. Faulkner, G., Pallavicini, A., Formentin, E., Comelli, A., Ievolella, C., Trevisan, S., Bortoletto, G., Scannapieco, P., Salamon, M., Mouly, V., Valle, G., and Lanfranchi, G. (1999) ZASP: a new Z-band alternatively spliced PDZ-motif protein, *J. Cell Biol. 146*, 465−475.
40. Zhou, Q., Ruiz-Lozano, P., Martone, M. E., and Chen, J. (1999) Cypher, a striated muscle-restricted PDZ and LIM domain-containing protein, binds to α-actinin-2 and protein kinase C, *J. Biol. Chem. 274*, 19807−19813.
41. Satoh, M., Takahashi, M., Sakamoto, T., Hiroe, M., Marumo, F., and Kimura, A. (1999) Structural analysis of the titin gene in hypertrophic cardiomyopathy: identification of a novel disease gene, *Biochem. Biophys. Res. Commun. 262*, 411−417.
42. Yajima, H., Ohtsuka, H., Kawamura, Y., Kume, H., Murayama, T., Abe, H., Kimura, S., and Maruyama, K. (1996) A 11.5-kb 5′-terminal cDNA of chicken connectin/titin reveals its Z-line binding region, *Biochem. Biophys. Res. Commun. 223*, 160−164.

BI002739R